

NRTSI: Non-Recurrent Time Series Imputation for Irregularly-sampled Data

Siyuan Shan¹ Junier B. Oliva¹

Abstract

Time series imputation is a fundamental task for understanding time series with missing data. Existing imputation methods often rely on recurrent models such as RNNs and ordinary differential equations, both of which suffer from the error compounding problems of recurrent models. In this work, we view the imputation task from the perspective of permutation equivariant modeling of sets and propose a novel imputation model called NRTSI without any recurrent modules. Taking advantage of the permutation equivariant nature of NRTSI, we design a principled and efficient hierarchical imputation procedure. NRTSI can easily handle irregularly-sampled data, perform multiple-mode stochastic imputation, and handle the scenario where dimensions are partially observed. We show that NRTSI achieves state-of-the-art performance across a wide range of commonly used time series imputation benchmarks.

1. Introduction

Time series imputation is a fundamental problem in spatiotemporal modeling that aims to recover the missing values of a partially observed time series. The problem of missing values is frequently encountered in real-life sequential data, e.g. trajectories often contain missing data due to unreliable sensors or object occlusion. To accurately recover missing values, machine learning models need to understand the underlying dynamics of a potentially complex system.

Time series imputation problems have been studied for decades. Modern approaches tackle time series imputation problems in a data-driven fashion. For example, generative adversarial networks (GAN) are used to impute missing values in (Luo et al., 2018a) and recurrent neural networks (RNNs) are used in (Che et al., 2018; Cao et al., 2018). However, these methods are all recurrent, which means that

¹Department of Computer Science, University of North Carolina at Chapel Hill. Correspondence to: Siyuan Shan <siyuan-shan@cs.unc.edu>.

the value at the current timestep is predicted based on the imputed values at the previous timesteps. Hence, recurrent models are highly susceptible to the error compounding problem, which can become catastrophic for long-range sequence modeling. To solve this problem, NAOMI (Liu et al., 2019) uses a divide and conquer procedure to impute missing values hierarchically from coarse to fine. Despite the non-recurrent imputation procedure, NAOMI still relies on recurrent modules like RNNs to process input data, which are sensitive to sequence lengths and unable to directly process irregularly-sampled time series as RNNs assume a constant time interval between observations.

Several works have considered irregularly-sampled time series. For example, (Che et al., 2018) proposed GRU-D, which adds a decay mechanism to standard GRU. Another line of work (Rubanova et al., 2019; De Brouwer et al., 2019; Kidger et al., 2020) employ the recently proposed Neural Ordinary Differential Equations (NeuralODE) (Chen et al., 2018) to handle irregularly-sampled time series. However, these works still suffer from error compounding problems due to their recurrent nature as shown in our experiments.

In this work, we propose NRTSI, a Non-Recurrent Time Series Imputation model. One of our key insights is that when imputing missing values in time series, the valuable information from the observed sequence is *what happened and when*. That is, for the imputation of missing timesteps, we must consider the context of all the observed values and when they were observed. This observed context is most naturally represented as a set of (time, data) tuples. To embed the tuples, we propose to employ permutation equivariant models, which respect the unordered nature of the tuple set. This is in stark contrast to previous works (e.g. NAOMI (Liu et al., 2019)), which embed observed points recurrently in a way that unnecessarily couples the temporal information (when things happened) with the order that points are processed. NRTSI provides two immediate advantages to recurrent embeddings. First, it can handle irregularly-sampled data (i.e. non-grid timesteps) as it decouples the temporal information and processes arbitrary times in the (time, data) tuples. Second, it allows one to impute multiple points in parallel thanks to its non-recurrent nature.

Our contributions are: (1) We propose a time series imputation model NRTSI from the perspective of set modeling.

(2) We propose an effective hierarchical imputation strategy that takes advantage of the non-recurrent nature of NRTSI and imputes data in a multiresolution fashion. (3) NRTSI is widely applicable to irregularly-sampled data, perform stochastic imputation, and data with partially observed dimensions. (4) Experiments on a wide range of datasets show that NRTSI achieves state-of-the-art imputation performance. Codes will be released upon publication.

2. Related Work

Missing Value Imputation Existing missing value imputation approaches roughly fall into two categories: statistical methods and deep generative models. Statistical methods often impose strong assumption on the missing patterns and design some hand-crafted rules such as mean-median averaging (Acuna & Rodriguez, 2004), linear regression (Ansley & Kohn, 1984), MICE (Azur et al., 2011) and k-nearest neighbours (Friedman et al., 2001). Though effective on simple tasks, these methods fail on more complicated scenarios where the missing patterns vary from task to task. Deep generative models offer a flexible framework for missing data imputation. For example, (Che et al., 2018; Cao et al., 2018; Choi et al., 2021) propose variants of RNNs to impute time series. Generative adversarial networks are leveraged in (Fedus et al., 2018; Yoon et al., 2018; Luo et al., 2018b). However, all of these works are recurrent.

NAOMI (Liu et al., 2019) performs time series imputation via a non-recurrent imputation procedure that imputes from coarse to fine-grained resolutions using a divide-and-conquer strategy. However, NAOMI relies on bidirectional RNNs to process observed time points, which limits its application for irregularly-sampled time data and loses the opportunity to efficiently impute multiple time points in parallel. Moreover, the hierarchical imputation procedure of NAOMI assumes that the multivariate data at a timestep is either completely observed or completely missing along all the dimensions. In contrast, the imputation procedure of NRTSI also works well when dimensions are partially observed. CDSA (Ma et al., 2019) performs time series imputation via self-attention without recurrent modules. However, CDSA is specifically designed for geo-tagged data, unable to tackle irregularly-sampled data, and does not exploit the multiresolution information.

Irregularly-sampled Time Series RNN is the dominant model for high-dimensional, regularly-sampled time series. However, it is not an appropriate fit for irregularly-sampled time series. A standard trick for applying RNNs to irregular time series is to divide the timeline into equally-sized intervals and impute or aggregate observations using averages (Lipton et al., 2016). However, such preprocessing loses information, especially about the timing of measurements

for accurate predictions.

To solve this problem, several recent works (Rajkomar et al., 2018; Che et al., 2018) propose variants of RNNs with continuous dynamics given by a simple exponential decay between observations. These models are further improved by NeuralODE (Chen et al., 2018) based methods that learn the continuous dynamics rather than using hand-crafted exponential decay rules. For example, ODE-RNN (Rubanova et al., 2019; De Brouwer et al., 2019) models the latent dynamics using ODE and update the latent state at observations. This line of works is improved by NeuralCDE (Kidger et al., 2020) that enables the latent state to have a continuous dependency on the observed data via controlled differential equations (Lyons et al., 2007). Despite the success of these continuous variants of RNNs for irregular time series analysis, these models inherit the recurrent nature of RNNs. Even though the gradient explosion/vanishing problem of ODE-RNN is mitigated by introducing forgetting gates to NeuralODE (Lechner & Hasani, 2020), these models still suffer from the error compounding problems.

Another way to model irregularly-sampled time series is to use a time encoding function (Xu et al., 2019) and view a temporal sequence as an unordered set (Kim et al., 2018; Horn et al., 2020), where each set element is a tuple that contains the observed data $\mathbf{x}_t \in \mathbb{R}^d$ at timestep $t \in \mathbb{R}$ and the encoding of the time stamp $\phi(t)$. As t is a real-valued scalar rather than an integer, this form of representation can handle irregularly-sampled time series. Similar to SeFT (Horn et al., 2020) and Attentive Neural Process (ANP) (Kim et al., 2018), we also regard time points as an unordered set. However, only time series classification is considered in (Xu et al., 2019; Horn et al., 2020) while we target at time series imputation. Though ANP is applicable for the imputation task, the information of what timesteps to impute (target input) is not utilized when ANP uses self-attention to compute the representations of observed data (context input/output pairs). As a result, the representations might be suboptimal as the self-attention network does not know at what time stamps we want to impute. Moreover, ANP does not exploit the multiresolution information of sequence data. These two weaknesses lead to worse performance as shown in our experiments.

3. Methods

3.1. Preliminaries

In this section, we present the necessary preliminaries to formulate the sequence imputation task from the perspective of set modeling. A set is a collection that does not impose order among its elements. We denote a set as $\mathbf{X} = \{\mathbf{x}_i\}_{i=1}^N$ with the set element $\mathbf{x}_i \in \mathcal{X}$.

Permutation Equivariant and Permutation Invariant, as de-

8	7	6	5	4	3	2	1	0	1	2	3	4	5	4	3	2	1	0	1	2	3	4	5	6	7	8	9	10	11	12	13	14	15	16
8	7	6	5	4	3	2	1	0	1	2	3	4	5	4	3	2	1	0	1	2	3	4	5	6	7	8	7	6	5	4	3	2	1	0
0	1	2	3	4	3	2	1	0	1	2	3	4	5	4	3	2	1	0	1	2	3	4	3	2	1	0	1	2	3	4	3	2	1	0
0	1	2	3	4	3	2	1	0	1	2	2	1	0	1	2	2	1	0	1	2	3	4	3	2	1	0	1	2	3	4	3	2	1	0
0	1	2	1	0	1	2	1	0	1	2	2	1	0	1	2	2	1	0	1	2	1	0	1	2	1	0	1	2	1	0	1	2	1	0
0	1	0	1	0	1	0	1	0	1	0	0	1	0	1	0	0	1	0	1	0	1	0	1	0	1	0	1	0	1	0	1	0	1	0
0	0	0	0	0	0	0	0	0	0	0	0	0	0	0	0	0	0	0	0	0	0	0	0	0	0	0	0	0	0	0	0	0	0	0

Figure 1. Illustration of the imputation procedure. Blue, green and red boxes respectively represent missing data, observed data, and data to impute next. Numbers inside each box represent the missing gap to the closest observed data and we assume the missing gap of observed data to be 0. Given a time series with 2 observed values and 32 missing values, the imputation procedure starts at the first row and ends at the bottom row where all data are imputed.

fined below, are two well-known terminologies for sets.

Definition 1 (Permutation Equivariant) Let $f : \mathcal{X}^N \rightarrow \mathcal{Y}^N$ be a function, then f is permutation equivariant iff for any permutation $\pi(\cdot)$, $f(\pi(\mathbf{X})) = \pi(f(\mathbf{X}))$.

Definition 2 (Permutation Invariant) Let $f : \mathcal{X}^N \rightarrow \mathcal{Y}$ be a function, then f is permutation invariant iff for any permutation $\pi(\cdot)$, $f(\pi(\mathbf{X})) = f(\mathbf{X})$.

We denote a time series with N observations as a set $\mathbf{S} = \{\mathbf{s}_i\}_{i=1}^N$, each observation \mathbf{s}_i is a tuple (t_i, \mathbf{x}_i) , where $t_i \in \mathbb{R}^+$ denotes the observation time and $\mathbf{x}_i \in \mathbb{R}^d$ represents the observed data. Given an observed time series \mathbf{S} , we aim to impute the missing data based on \mathbf{S} . We also organize data to impute as a set $\hat{\mathbf{S}} = \{\hat{\mathbf{s}}_j\}_{j=1}^M$, where M is the number of missing data. Each set elements $\hat{\mathbf{s}}_j$ is a tuple $(\hat{t}_j, \Delta\hat{t}_j)$, where $\hat{t}_j \in \mathbb{R}^+$ is a timestep to impute and $\Delta\hat{t}_j \in \mathbb{R}^+$ denotes the missing gap (i.e. the time interval length between \hat{t}_j and its closest observation time in \mathbf{S}). Formally, $\Delta\hat{t}_j$ can be defined as $\Delta\hat{t}_j = \min_{(t_i, \mathbf{x}_i) \in \mathbf{S}} |t_i - \hat{t}_j|$. Note that both \hat{t}_j and t_i are real-valued scalars as our model is designed to impute observations at arbitrary irregularly-sampled timesteps rather than fixed grid points.

The missing gap information is essential for our hierarchical imputation procedure. As will be discussed in details in Sec 3.2, we select a subset $\mathbf{G} \subseteq \hat{\mathbf{S}}$ to impute every time based on the missing gap information. We denote the imputation result as $\mathbf{H} = \{\mathbf{h}_j\}_{j=1}^{|\mathbf{G}|}$ with $\mathbf{h}_j \in \mathbb{R}^d$. \mathbf{H} is computed using a imputation model f as $\mathbf{H} = f(\mathbf{G}; \mathbf{S})$.

To respect the unordered nature of sets, we employ a f that is permutation equivariant w.r.t. \mathbf{G} and permutation invariant w.r.t. \mathbf{S} , i.e.

$$\rho(\mathbf{H}) = f(\rho(\mathbf{G}); \pi(\mathbf{S})), \quad (1)$$

where π and ρ represent two arbitrary permutation operators.

3.2. Hierarchical Imputation

In this section, we discuss our proposed hierarchical imputation procedure given trained imputation models. We will discuss the imputation models in Sec 3.3.

Exploiting the hierarchical structures of data is pivotal for

the success of numerous generation models (Karras et al., 2018; Liu et al., 2018). NAOMI (Liu et al., 2019) exploits the multiresolution structures of spatiotemporal data for time series imputation. The design philosophy of NAOMI’s imputation procedure is to always impute the missing data with the largest missing gap first. Unfortunately, the way NAOMI is implemented violates its design philosophy due to its reliance on RNNs. For RNNs, it is impossible to directly obtain the latent vector in the middle part of a time series without visiting the start or the end of this time series first. As a result, NAOMI has to first impute the missing data located between the two leftmost observed data, even in the case where the missing data with the largest missing gap locates in the middle of the time series.

By regarding the observed sequence data as a set, which frees us from the sequential constraint of RNNs, our model can directly impute missing data at any desired time point. Furthermore, the non-recurrent nature enables us to impute multiple missing data with similar missing gaps in parallel,

Algorithm 1 IMPUTATION PROCEDURE

Require: f_θ^l : imputation model at resolution level l , L : the maximum resolution level, \mathbf{S} : observed data, $\hat{\mathbf{S}}$: data to impute

- 1: Initialize current imputation set \mathbf{G} as an empty set, i.e. $\mathbf{G} \leftarrow \emptyset$, initialize current resolution level l to L , i.e. $l \leftarrow L$
- 2: **while** $\hat{\mathbf{S}}$ is not empty **do**
- 3: Find times points to impute at current level $\hat{\mathbf{S}}^l \leftarrow \{(\hat{t}_j, \Delta\hat{t}_j) \mid (\hat{t}_j, \Delta\hat{t}_j) \in \hat{\mathbf{S}} \text{ and } [2^{l-1}] < \Delta\hat{t}_j \leq 2^l\}$
- 4: **if** $\hat{\mathbf{S}}^l$ is not empty **then**
- 5: Find the data to impute with the largest missing gap and put them into \mathbf{G} , i.e. $\mathbf{G} \leftarrow \{(\hat{t}_j, \Delta\hat{t}_j) \mid (\hat{t}_j, \Delta\hat{t}_j) \in \hat{\mathbf{S}}^l, \Delta\hat{t}_j = \max_j \Delta\hat{t}_j\}$
- 6: Compute the imputation results $\mathbf{H} = \{(\hat{t}_j, \mathbf{h}_j)\}_{j=1}^{|\mathbf{G}|}$ based on the observed data \mathbf{S} , i.e. $\mathbf{H} \leftarrow f_\theta^l(\mathbf{G}; \mathbf{S})$
- 7: Regard imputed data as observed data and delete them from $\hat{\mathbf{S}}$, i.e. $\mathbf{S} \leftarrow \mathbf{S} \cup \mathbf{H}, \hat{\mathbf{S}} \leftarrow \hat{\mathbf{S}} \setminus \mathbf{G}$
- 8: Update the missing gap information in $\hat{\mathbf{S}}$
- 9: **else**
- 10: $l \leftarrow l - 1$
- 11: **end if**
- 12: **end while**
- 13: **return** Imputation result \mathbf{S}

which is impossible for recurrent models.

We impute unobserved data with the largest missing gap (high resolution level) first and regard the imputed data as observed data, based on which we impute the remaining missing data with smaller missing gaps (low resolution level). Every resolution level is taken care of by a corresponding imputation model. Details of our imputation procedure are given in Algorithm 1 and an example of the procedure is given in Figure 1. As shown in Figure 1, our model can impute multiple missing data in parallel, which is more efficient than NAOMI. Note that our model can handle irregularly-sampled data, though we only show the imputation procedure where data are observed at integer timesteps in Figure 1.

3.3. Imputation Model

In this section, we describe how we design and train the imputation model f_θ . Theoretically, any permutation equivariant model is appropriate. Representative models include DeepSets (Zaheer et al., 2017), ExNODE (Li et al., 2020) and Transformers (Vaswani et al., 2017; Lee et al., 2019). In this work, we adopt the multihead self-attention mechanism in Transformers for its strong capacity to model the high-order interactions between the elements in \mathbf{G} and \mathbf{S} .

Time Encoding Function Transformers do not require that the sequential data be processed in sequential order. Originally, the input to Transformers was a set of unordered elements and every element consists of a word embedding vector and a position encoding vector. Though the inputs are unordered, Transformers are aware of the position information of word embeddings given by the position encoding vectors.

Similar to the position encoding operator in Transformers, we use the time encoding function ϕ proposed by (Horn et al., 2020) to transform a time stamp $t \in \mathbb{R}^+$ to a time encoding vector $z = \phi(t) \in \mathbb{R}^\tau$, where

$$\begin{aligned} z_{2k}(t) &:= \sin\left(\frac{t}{\nu^{2k/\tau}}\right) \\ z_{2k+1}(t) &:= \cos\left(\frac{t}{\nu^{2k/\tau}}\right) \end{aligned} \quad (2)$$

with $k \in \{0, \dots, \tau/2\}$, τ denoting the dimensionality of the encoding vector and ν representing the maximum time scale that is expected in the data.

Note that in Eq. (2), we are using the absolute time information, which seems less meaningful than the relative time information for imputation. However, as pointed out in (Vaswani et al., 2017), the sinusoid functions allow the model to easily learn to attend by relative positions since for any fixed offset Δt , $\phi(t + \Delta t)$ can be represented as a linear function of $\phi(t)$. We show this property in the Appendix.

In practice, we find the absolute time encoding works well for all the experiments considered in this paper.¹

Data Representation Recall that in Algorithm 1, our model maps a collection of time stamps to impute \mathbf{G} into a set of corresponding imputed data \mathbf{H} conditioned on the observed data \mathbf{S} , i.e. $\mathbf{H} = f_\theta^l(\mathbf{G}; \mathbf{S})$. An element \mathbf{s}_i in \mathbf{S} contains the information of the observation time t_i and the observed data \mathbf{x}_i . In our model, \mathbf{s}_i is represented as $\mathbf{s}_i = [\mathbf{x}_i, \phi(t_i), 1] \in \mathbb{R}^{d+\tau+1}$, where ϕ is the time encoding function in Eq. (2), $[\cdot, \cdot]$ is a concatenation operator and 1 is a scalar that informs our model \mathbf{s}_i represents an observed data rather than a missing data. Then, we concatenate all elements in \mathbf{S} as $\mathbf{S} = [\mathbf{s}_{\pi_1}, \mathbf{s}_{\pi_2}, \dots, \mathbf{s}_{\pi_{|\mathbf{S}|}}] \in \mathbb{R}^{|\mathbf{S}| \times (d+\tau+1)}$, where π denotes arbitrary permutation. We include π to emphasize that the imputation result is invariant to the order that the observation data is presented to our model.

An element \mathbf{g}_j in \mathbf{G} contains the timesteps to impute and is represented as $\mathbf{g}_j = [\mathbf{0}, \phi(t_j), 0] \in \mathbb{R}^{d+\tau+1}$, where $\mathbf{0} \in \mathbb{R}^d$ is a zero vector since the data is missing and 0 is a scalar that informs our model this elements represents a data to impute. Then we also concatenate all elements in \mathbf{G} in arbitrary order as $\mathbf{G} = [\mathbf{g}_{\rho_1}, \mathbf{g}_{\rho_2}, \dots, \mathbf{g}_{\rho_{|\mathbf{G}|}}] \in \mathbb{R}^{|\mathbf{G}| \times (d+\tau+1)}$ where ρ denotes another arbitrary permutation operator irrelevant to π .

Computation Steps We concatenate \mathbf{S} and \mathbf{G} as the input to the model, i.e. $[\mathbf{S}, \mathbf{G}] \in \mathbb{R}^{(|\mathbf{S}|+|\mathbf{G}|) \times (d+\tau+1)}$. We obtain the imputation results \mathbf{H} via a permutation equivariant model f as $\mathbf{H} = f([\mathbf{S}, \mathbf{G}])$ with the following steps:

$$\begin{aligned} [\mathbf{S}^{(1)}, \mathbf{G}^{(1)}] &= f_{\text{in}}([\mathbf{S}, \mathbf{G}]) \\ [\mathbf{S}^{(2)}, \mathbf{G}^{(2)}] &= f_{\text{enc}}([\mathbf{S}^{(1)}, \mathbf{G}^{(1)}]) \\ \mathbf{H} &= f_{\text{out}}(\mathbf{G}^{(2)}) \end{aligned} \quad (3)$$

First, a linear layer $f_{\text{in}} : \mathbb{R}^{d+\tau+1} \rightarrow \mathbb{R}^{d_h}$ maps the input data to a high-dimensional space. Then, a Transformer encoder $f_{\text{enc}} : \mathbb{R}^{d_h} \rightarrow \mathbb{R}^{d_h}$ with alternative multi-head self-attention sublayers and feedforward sublayers is used to model the interactions between $\mathbf{S}^{(1)}$ and $\mathbf{G}^{(1)}$. Finally, the imputation result $\mathbf{H} = [\mathbf{h}_{\rho_1}, \mathbf{h}_{\rho_2}, \dots, \mathbf{h}_{\rho_{|\mathbf{G}|}}] \in \mathbb{R}^{|\mathbf{G}| \times d}$ is obtained via another linear layer $f_{\text{out}} : \mathbb{R}^{d_h} \rightarrow \mathbb{R}^d$ that is only applied on $\mathbf{G}^{(2)}$. The architecture of the imputation model is illustrated in Figure 2.

As the set elements are individually transformed by the linear layers and the attention mechanism in f_{enc} is a weighted sum over all set elements, the whole model f is permutation

¹It might be beneficial to incorporate relative position information to our model as done in (Shaw et al., 2018; Huang et al., 2018; Raffel et al., 2020; Ke et al., 2021). However, these works assume a constant position interval between words, which is not directly applicable to the imputation task for irregularly-sampled data. We leave the exploration of this direction as to future work.

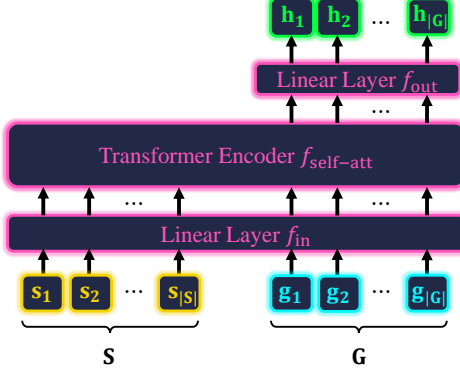


Figure 2. Illustration of the imputation model.

equivariant w.r.t. \mathbf{G} and the imputation result corresponding to each timestep is invariant to the order that elements in \mathbf{S} are fed into f . This property is concisely shown by Eq. (1).

Training Objective We denote our imputation model with learnable parameters θ at level l as f_θ^l , which include the two linear layers and the Transformer encoder. Our model is trained by optimizing the following objective

$$\min_{\theta} \mathbb{E}_{\mathbf{G} \sim p(\mathbf{G}), \mathbf{S} \sim p(\mathbf{S}), \mathbf{Y} \sim p(\mathbf{Y})} \left[\frac{1}{|\mathbf{G}|} \sum_{j=1}^{|\mathbf{G}|} \mathcal{L}(\mathbf{h}_j, \mathbf{y}_j) \right], \quad (4)$$

where $\mathbf{h}_j \in \mathbf{H} = f_\theta^l(\mathbf{G}; \mathbf{S})$ is an imputed data and $\mathbf{y}_j \in \mathbf{Y}$ denotes the corresponding ground truth imputation target. For deterministic datasets, we use Mean Square Error (MSE), i.e. $\mathcal{L}(\mathbf{h}_j, \mathbf{y}_j) = \|\mathbf{h}_j - \mathbf{y}_j\|_2^2$. For stochastic datasets, we minimize the negative log-likelihood of a Gaussian distribution with diagonal covariance, i.e.

$$\mathcal{L}(\mathbf{h}_j, \mathbf{y}_j) = -\log \mathcal{N}(\mathbf{y}_j | \mu(\mathbf{h}_j), \text{diag}(\sigma(\mathbf{h}_j))), \quad (5)$$

where $\mu : \mathbb{R}^d \rightarrow \mathbb{R}^d$ and $\sigma : \mathbb{R}^d \rightarrow \mathbb{R}^d$ are two linear layers.

Similar to NAOMI, we find a single model struggles at imputing at all resolution levels. Therefore, we train multiple models f_θ^l sequentially from level 1 to level L . When we start training on level $l+1$, we adopt the transfer learning strategy to initialize the parameters of f_θ^{l+1} from the trained weights of model f_θ^l . The assumption is that the trained lower-level model already captures the dynamics at a fine-grained scale, and it is beneficial to train higher-level models based on the prior knowledge of lower-level dynamics.

It is important for a machine learning model to have consistent training and inference configurations to achieve the desired performance. Therefore, when training our model, we follow a similar procedure in Algorithm 1. The only difference during training is at line 7 of Algorithm 1, where we regard the ground truth imputation target \mathbf{Y} as observed

data for the subsequent training steps rather than the imputation result \mathbf{H} . This idea is similar to the Teacher Forcing algorithm (Williams & Zipser, 1989) commonly used to stabilize and speed up the training of RNNs. Details of the training procedure are given in the Appendix.

3.4. Model Variants

In this section, we introduce three variants of our model to tackle irregularly-sampled data, generate multiple-mode stochastic imputations, and handle multivariate sequence with partially observed dimensions.

Irregularly-sampled Data Only a small modification of Algorithm 1 is needed to handle irregularly-sampled data. At line 5, we may find multiple data with the largest missing gap to impute in parallel for regularly-sampled data. However, for irregularly-sampled data, it is very likely that we can only find one data to impute, which could slow down the imputation process. Therefore, we modify the way to obtain \mathbf{G} as follows

$$\mathbf{G} \leftarrow \{ (\hat{t}_j, \hat{\Delta t}_j) \mid (\hat{t}_j, \hat{\Delta t}_j) \in \hat{\mathbf{S}}^l, \hat{\Delta t}_j \in (a, b] \}, \quad (6)$$

$$a = \max_j \hat{\Delta t}_j - \Delta, b = \max_j \hat{\Delta t}_j,$$

where $\Delta \in \mathbb{R}^+$ is a hyperparameter. In this way, we can collect multiple data into \mathbf{G} with missing gaps in the Δ -vicinity to the maximum missing gap $\max_j \hat{\Delta t}_j$.

Stochastic Imputation For deterministic datasets (e.g. billiard trajectories), we can impute all data in \mathbf{G} simultaneously due to the lack of stochasticity. However, for stochastic datasets (e.g. football player trajectories), the imputation results at different timesteps may be incongruous if we sample them simultaneously from their corresponding distributions in Eq. (5). This problem is caused by the independence assumption resulting from the parallel and independent sampling.

Empirically, we observe that uncertainty is primarily in data with large missing gaps, while for data with small missing gaps there is almost no stochasticity. Based on this observation, we propose to impute data with large missing gaps one-by-one and impute data with small missing gaps simultaneously in parallel. In practice, we find this modification does not significantly slow down the imputation process as there are much fewer data with large missing gaps compared to those with small missing gaps.

Partially Observed Dimensions The discussion so far assumes that the multivariate data at a timestep is either completely observed or completely missing along all the dimensions. However, a timestep may be only partially observed (with a subset of features missing at that time). To tackle this scenario, we also propose to use a hierarchical

Table 1. Quantitative comparison on Billiards dataset. Statistics closer to the expert indicate better performance.

Models	Linear	KNN	GRUI	MaskGAN	SingleRes	NAOMI	Ours	Expert
Sinuosity	1.121	1.469	1.859	1.095	1.019	1.006	1.003	1.000
step change ($\times 10^{-3}$)	0.961	24.59	28.19	15.35	9.290	7.239	5.621	1.588
reflection to wall	0.247	0.189	0.225	0.100	0.038	0.023	0.021	0.018
L2 loss ($\times 10^{-2}$)	19.00	5.381	20.57	1.830	0.233	0.067	0.024	0.000

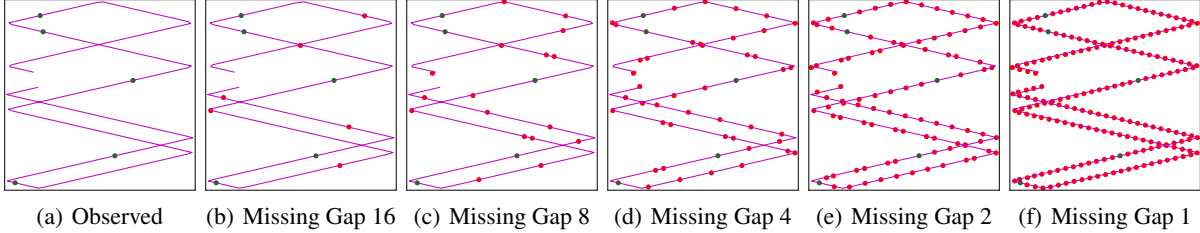


Figure 3. Imputation procedure on the Billiards dataset. The red points denote imputed data while the green points denote observed data. The purple solid line is the ground-truth trajectory. The initial observed data is shown in (a), the imputed data with missing gaps 16 to 1 are shown in (b)-(f). We omit the intermediate results at missing gaps 15, 13, 7, 6, and 3 due to the limitation of space.

imputation strategy. However, missing gaps may no longer be the driving factor for an effective imputation order, as the number of dimensions observed may affect the effectiveness of imputations. Therefore, we modify Algorithm 1 to impute the timesteps with the most missing dimensions first rather than the timesteps with the largest missing gap. We also modify how data are represented to our model as $[\mathbf{x}_i, \phi(t_i), \mathbf{m}_i] \in \mathbb{R}^{d+\tau+d}$ where $\mathbf{m}_i \in \{0, 1\}^d$ is an observation mask that informs the model which dimensions are observed and which are not.

4. Experiment

We evaluate NRTSI on popular time series imputation benchmarks against strong baselines. We also conduct extensive experiments to test whether NRTSI can handle irregularly-sampled data, generate stochastic trajectories, and handle the scenario where dimensions are partially observed. *An extensive hyperparameter search is performed for all the methods. Please refer to the Appendix for the discussions of model architecture, training, ablation studies, additional visualization results, and baseline hyperparameter search.*

4.1. Billiards Ball Trajectory

Dataset Billiards dataset (Salimans & Kingma, 2016) contains 4,000 training and 1,000 testing regularly-sampled sequences of Billiards ball trajectories in a rectangular world. Each ball is initialized with a random position and a random velocity and rolled-out for 200 timesteps. All balls have a fixed size and uniform density, and there is no friction.

Results We train on this dataset using MSE loss and evaluate via the L_2 loss between imputed values and ground-truth. We also use another three metrics *Sinuosity*, *step change*

and *reflection to wall* defined in (Liu et al., 2019) to evaluate the realism of the imputed trajectories.

We compare NRTSI with NAOMI as well as its baselines. Please refer to (Liu et al., 2019) for detailed information about these baselines. Quantitative results are reported in Table 1, where Expert denotes the ground truth trajectories; statistics closer to the expert are better. To calculate the statistics in Table 1, we follow (Liu et al., 2019) and randomly select 180 to 195 timesteps and regard them as missing for each trajectory. The test set is repeated 100 times to make sure the statistics consider a variety of missing patterns. Our method reduces the L_2 loss by 64% compared to NAOMI and compares favorably to the baselines on all metrics except *step change*, as linear interpolation maintains a constant step size change by design.

We visualize the imputation procedure in Figure 3. With only five points observed (shown in green), our model imputes the data with the largest missing gap (16) first, based on which it hierarchically imputes the remaining data with smaller missing gaps. The final imputed trajectory not only aligns closely with the ground truth trajectory but also maintains a constant speed and straight lines between collisions. To better understand how NRTSI imputes missing data, we

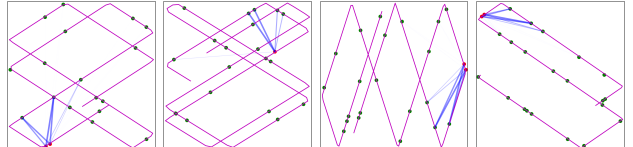


Figure 4. Visualization of an attention head. Red points are the imputed data, green points are the observed data. The softmax attention weights are visualized via the blue lines. The wider and less transparent blue lines are, the larger the attention weights.

Table 2. Traffic data L2 loss ($\times 10^{-4}$) comparison.

Linear	GRUI	KNN	MaskGAN	SingleRes	NAOMI	Ours
15.59	15.24	4.58	6.02	4.51	3.54	3.22

also visualize the attention maps of an attention head in NRTSI in Figure 4 where this attention head models short-range interactions in a single direction. We show more attention patterns captured by other heads in the Appendix.

4.2. Traffic Time Series

Dataset The PEMS-SF traffic (Dua & Graff, 2017) dataset contains 267 training and 173 testing regularly-sampled sequences of length 144 (sampled every 10 mins throughout the day). It is multivariate with 963 dimensions, representing the freeway occupancy rate from 963 sensors.

Results We train on this dataset using MSE loss and evaluate using the same set of baselines as the Billiards dataset. Following (Liu et al., 2019), we repeat the testing set 100 times and randomly generate a masking sequence for each time series with 122 to 140 missing values. The $L2$ losses of all methods are reported in Table 2, and our method outperforms the baselines.

4.3. MuJoCo Physics Simulation

Dataset This is a physical simulation dataset created in (Rubanova et al., 2019) using the “Hopper” model from the Deepmind Control Suite (Tassa et al., 2018). Initial positions and velocities of the hopper are randomly sampled such that the hopper rotates in the air and falls on the ground. The dataset is 14-dimensional and contains 10,000 sequences of 100 regularly-sampled time points each.

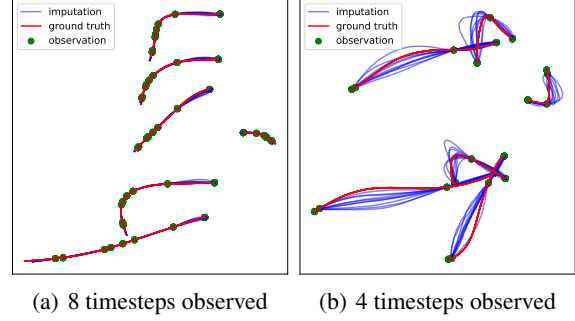
Results We train on this dataset using MSE loss and compare NRTSI to the state-of-the-art method Latent-ODE (Rubanova et al., 2019) as well as its baseline methods and NAOMI (Liu et al., 2019). We report the MSEs with different observation rates in Table 3. Our method compares favorably to Latent-ODE with 20%, 30% and 50% observed data. When only 10% data are observed, NRTSI is comparable to Latent-ODE and NAOMI.

4.4. Football Player Trajectory

Dataset Next we consider a football player trajectory dataset from the 2021 Big Data Bowl data (Kaggle, 2020).

Table 3. MuJoCo Simulation Data MSE loss (10^{-3}) comparison.

Method	10%	20%	30%	50%
RNN GRU-D	19.68	14.21	11.34	7.48
ODE-RNN	16.47	12.09	9.86	6.65
Latent-ODE	3.60	2.95	3.00	2.85
NAOMI	4.42	2.32	1.46	0.93
Ours	4.06	1.22	0.63	0.26



(a) 8 timesteps observed

(b) 4 timesteps observed

Figure 5. Trajectories of six offensive football players. Green points are observed locations, red lines are ground truth trajectories, and blue lines are imputations sampled independently.

This dataset contains 9,543 time series with 50 regularly-sampled time points each. The sampling rate is 10 Hz. Each time series contains the 2D trajectories of six offensive players and is therefore 12-dimensional. During training and testing, we treat all players in a time series equally and randomly permute their orders. 8,000 time series are randomly selected for training and the others are used for testing.

Evaluation Metrics This dataset is stochastic and contains multiple modes since there are multiple possible player trajectories based on sparsely observed data. Therefore, we follow (Park et al., 2020) to use $minMSE$ to evaluate the precision and the ratio between $avgMSE$ and $minMSE$ to evaluate the diversity of the imputed trajectories. $minMSE$ and $avgMSE$ respectively denote the minimum and average MSEs between the ground truth and n independently sampled imputation trajectories. A small $minMSE$ indicates that at least one of n samples has high precision, while a large $avgMSE$ implies that these n samples are spread out. From this observation, we use $avgMSE / minMSE$ to measure the diversity of samples. We also follow (Liu et al., 2019) to use *average trajectory length* and *step change* measure the quality of sampled trajectories.

Results We train on this dataset via minimizing the negative log-likelihood in Eq. (5). We randomly select 40 to 49 timesteps and regard them as missing for each trajectory. According to the discussion in Sec 3.4, data with missing gaps larger than 8 are imputed by sampling from the predicted distribution one-by-one while the others are imputed with the predicted mean values in parallel. As shown in

Table 4. Quantitative comparison on Football Player Trajectory. A larger $avgMSE / minMSE$ indicate better diversity. Other statistics closer to the expert indicate better performance.

Models	NAOMI	Ours	Expert
step change ($\times 10^{-3}$)	3.227	2.370	2.482
avg length	0.236	0.173	0.173
$minMSE$ ($\times 10^{-3}$)	4.079	1.908	0.000
$avgMSE / minMSE$	1.12	2.09	—
Imputation Time (s)	6.07	5.41	—

Table 4, NRTSI compares favorably to NAOMI, which is the state-of-the-art method on this kind of task. NRTSI also impute faster as it only takes 5.41 seconds to impute a batch of data with batch size 64 while NAOMI takes 6.07 seconds. *minMSE* and *avgMSE* are calculated from 10 independent samples. We qualitatively show the imputed trajectories in Figure 5. With more timesteps observed, there is less variance. When there are only a few observed data, our model can impute multiple realistic and reasonable trajectories.

4.5. Irregularly-sampled Data

We first test NRTSI on a toy example where the task is to impute sinusoidal functions. We follow (Rubanova et al., 2019) to create a irregularly-sampled dataset containing 1,000 sinusoidal functions with 100 time points in each. To test the imputation performance, we randomly select 90 timesteps for each function as missing data. Both Latent-ODE (Rubanova et al., 2019) and NRTSI capture the periodic pattern of this dataset, but NRTSI is much more accurate by achieving a MSE of 7.17×10^{-4} while Latent-ODE only achieves 5.05×10^{-2} .

Then, we evaluate NRTSI on an irregularly-sampled Billiards dataset. This dataset is created with the same parameters (e.g. initial ball speed range, travel time) to create its regularly-sampled counterpart in Sec 4.1. The only difference is that this dataset is irregularly-sampled. On this dataset, we compare NRTSI to two representative ODE methods for handling irregularly-sampled data, namely Latent-ODE (Rubanova et al., 2019) and NeuralCDE (Kidger et al., 2020), as well as a variant of NAOMI (Liu et al., 2019) we called NAOMI- Δ_t where the time gap information between observations are provided to its RNN update function. We use NAOMI- Δ_t since the original NAOMI model cannot handle irregularly-sampled data. We also compare to Attentive Neural Process (ANP) (Kim et al., 2018) which can handle irregularly-sampled data as ANP simply encodes times as scalars. To report the performance in Table 5, we randomly select 180 to 195 timesteps and regard them as missing for each trajectory. According to Table 5, NRTSI outperforms the baselines by a large margin despite extensive hyperparameter search for these baselines.

In practice, we find Latent-ODE is slow to train without rounding times to low-precision (e.g. one digit after the decimal point), and the rounding operation is harmful to the performance due to the loss of temporal precision. The slow training speed is caused by the frequent updates of the latent state at all unique times in a batch. For times with high

Table 5. L_2 loss on irregularly-sampled Billiards data ($\times 10^{-2}$).

Latent-ODE	NeuralCDE	ANP	NAOMI- Δ_t	Ours
52.42	34.01	29.31	1.121	0.042

Table 6. The MSE comparison under different missing rates on the air quality dataset and the gas sensor dataset.

Dataset	Method	missing rate							
		10%	20%	30%	40%	50%	60%	70%	80%
Air	BRITS	.1659	.2076	.2212	.2088	.2141	.2660	.2885	.3421
	RDIS	.1409	.1807	.2008	.1977	.2041	.2528	.2668	.3178
	Ours	.1230	.1155	.1189	.1250	.1297	.1378	.1542	.1790
Gas	BRITS	.0210	.0226	.0233	.0279	.0338	.0406	.0518	.1595
	RDIS	.0287	.0226	.0241	.0251	.0277	.0321	.0350	.0837
	Ours	.0165	.0195	.0196	.0229	.0286	.0311	.0362	.0445

precision without rounding, the number of unique times in a batch equals the batch size times the sequence length, which is too large for efficient training. NeuralCDE and ANP are efficient to train and perform well when the observation is dense. However, they fail when the observation becomes sparse as NeuralCDE is recurrent and ANP does not exploit the multiresolution information. As shown in Table 1 and Table 5, NRTSI respectively outperforms NAOMI on the regular and NAOMI- Δ_t on the irregular Billiards dataset, which indicates the general superiority of not using recurrent modules for imputation.

4.6. Partially Observed Dimensions

Air quality dataset (Zhang et al., 2017) and gas sensor dataset (Burgués et al., 2018) are two popular datasets to evaluate the scenario where dimensions are partially observed. Data in the air quality dataset and the gas sensor dataset are 11-dimensional and 19-dimensional respectively. For both datasets, we select 48 consecutive timesteps to generate one regularly-sampled time series. We compare NRTSI to the state-of-the-art method RDIS (Choi et al., 2021) and its strongest baseline BRITS (Cao et al., 2018). To report the MSEs in Table 6, we randomly discard data along with all timesteps and all dimensions with several different missing rates and use the discarded data as the ground truth. NRTSI outperforms RDIS for all the missing rates on the air quality dataset and most of the missing rates on the gas sensor dataset.

5. Conclusion

We present NRTSI, the first model that tackles sequence imputation tasks from the view of permutation equivariant set modeling and avoids the sequential constraint and the error compounding problem of recurrent models. NRTSI is broadly applicable to numerous application scenarios where data are irregularly-sampled with arbitrary precision, stochastic, or have partially observed dimensions. Extensive experiments demonstrate that NRTSI outperforms state-of-the-art methods on eight commonly used time series imputation benchmarks.

References

Acuna, E. and Rodriguez, C. The treatment of missing values and its effect on classifier accuracy. In *Classification, clustering, and data mining applications*, pp. 639–647. Springer, 2004.

Ansley, C. F. and Kohn, R. On the estimation of arima models with missing values. In *Time series analysis of irregularly observed data*, pp. 9–37. Springer, 1984.

Azur, M. J., Stuart, E. A., Frangakis, C., and Leaf, P. J. Multiple imputation by chained equations: what is it and how does it work? *International journal of methods in psychiatric research*, 20(1):40–49, 2011.

Burgués, J., Jiménez-Soto, J. M., and Marco, S. Estimation of the limit of detection in semiconductor gas sensors through linearized calibration models. *Analytica chimica acta*, 1013:13–25, 2018.

Cao, W., Wang, D., Li, J., Zhou, H., Li, L., and Li, Y. Brits: Bidirectional recurrent imputation for time series. In *Advances in Neural Information Processing Systems*, pp. 6775–6785, 2018.

Che, Z., Purushotham, S., Cho, K., Sontag, D., and Liu, Y. Recurrent neural networks for multivariate time series with missing values. *Scientific reports*, 8(1):1–12, 2018.

Chen, R. T., Rubanova, Y., Bettencourt, J., and Duvenaud, D. K. Neural ordinary differential equations. In *Advances in neural information processing systems*, pp. 6571–6583, 2018.

Choi, T.-M., Kang, J.-S., and Kim, J.-H. Rdis: Random drop imputation with self-training for incomplete time series data. *AAAI*, 2021.

De Brouwer, E., Simm, J., Arany, A., and Moreau, Y. Gru-ode-bayes: Continuous modeling of sporadically-observed time series. In *Advances in Neural Information Processing Systems*, pp. 7379–7390, 2019.

Dua, D. and Graff, C. UCI machine learning repository, 2017. URL <http://archive.ics.uci.edu/ml>.

Fedus, W., Goodfellow, I., and Dai, A. M. Maskgan: Better text generation via filling in the_. *ICLR*, 2018.

Friedman, J., Hastie, T., and Tibshirani, R. *The elements of statistical learning*, volume 1. Springer series in statistics New York, 2001.

Horn, M., Moor, M., Bock, C., Rieck, B., and Borgwardt, K. Set functions for time series. In *International Conference on Machine Learning*, pp. 4353–4363. PMLR, 2020.

Huang, C.-Z. A., Vaswani, A., Uszkoreit, J., Simon, I., Hawthorne, C., Shazeer, N., Dai, A. M., Hoffman, M. D., Dinculescu, M., and Eck, D. Music transformer: Generating music with long-term structure. In *International Conference on Learning Representations*, 2018.

Kaggle. Nfl big data bowl 2021. <https://www.kaggle.com/c/nfl-big-data-bowl-2021>, 2020. Accessed: 2021-01-02.

Karras, T., Aila, T., Laine, S., and Lehtinen, J. Progressive growing of gans for improved quality, stability, and variation. *ICLR*, 2018.

Ke, G., He, D., and Liu, T.-Y. Rethinking the positional encoding in language pre-training. *ICLR*, 2021.

Kidger, P., Morrill, J., Foster, J., and Lyons, T. Neural controlled differential equations for irregular time series. *NeurIPS*, 2020.

Kim, H., Mnih, A., Schwarz, J., Garnelo, M., Esfandiari, A., Rosenbaum, D., Vinyals, O., and Teh, Y. W. Attentive neural processes. In *International Conference on Learning Representations*, 2018.

Lechner, M. and Hasani, R. Learning long-term dependencies in irregularly-sampled time series. *NeurIPS*, 2020.

Lee, J., Lee, Y., Kim, J., Kosiorek, A., Choi, S., and Teh, Y. W. Set transformer: A framework for attention-based permutation-invariant neural networks. In *International Conference on Machine Learning*, pp. 3744–3753. PMLR, 2019.

Li, Y., Yi, H., Bender, C., Shan, S., and Oliva, J. B. Exchangeable neural ode for set modeling. *Advances in Neural Information Processing Systems*, 33, 2020.

Lipton, Z. C., Kale, D., and Wetzel, R. Directly modeling missing data in sequences with rnns: Improved classification of clinical time series. In *Machine learning for healthcare conference*, pp. 253–270. PMLR, 2016.

Liu, P. J., Saleh, M., Pot, E., Goodrich, B., Sepassi, R., Kaiser, L., and Shazeer, N. Generating wikipedia by summarizing long sequences. In *International Conference on Learning Representations*, 2018.

Liu, Y., Yu, R., Zheng, S., Zhan, E., and Yue, Y. Naomi: Non-autoregressive multiresolution sequence imputation. In *Advances in Neural Information Processing Systems*, pp. 11238–11248, 2019.

Luo, Y., Cai, X., ZHANG, Y., Xu, J., and xiaojie, Y. Multivariate time series imputation with generative adversarial networks. In *Advances in Neural Information Processing Systems 31*, pp. 1596–1607. Curran Associates, Inc., 2018a.

Luo, Y., Cai, X., Zhang, Y., Xu, J., et al. Multivariate time series imputation with generative adversarial networks. In *Advances in Neural Information Processing Systems*, pp. 1596–1607, 2018b.

Lyons, T. J., Caruana, M., and Lévy, T. *Differential equations driven by rough paths*. Springer, 2007.

Ma, J., Shou, Z., Zareian, A., Mansour, H., Vetro, A., and Chang, S.-F. Cdsa: Cross-dimensional self-attention for multivariate, geo-tagged time series imputation. *arXiv preprint arXiv:1905.09904*, 2019.

Park, S. H., Lee, G., Bhat, M., Seo, J., Kang, M., Francis, J., Jadhav, A. R., Liang, P. P., and Morency, L.-P. Diverse and admissible trajectory forecasting through multimodal context understanding. *ECCV*, 2020.

Raffel, C., Shazeer, N., Roberts, A., Lee, K., Narang, S., Matena, M., Zhou, Y., Li, W., and Liu, P. J. Exploring the limits of transfer learning with a unified text-to-text transformer. *Journal of Machine Learning Research*, 21: 1–67, 2020.

Rajkomar, A., Oren, E., Chen, K., Dai, A. M., Hajaj, N., Hardt, M., Liu, P. J., Liu, X., Marcus, J., Sun, M., et al. Scalable and accurate deep learning with electronic health records. *NPJ Digital Medicine*, 1(1):18, 2018.

Rubanova, Y., Chen, R. T., and Duvenaud, D. Latent odes for irregularly-sampled time series. *NeurIPS*, 2019.

Salimans, T. and Kingma, D. P. Weight normalization: A simple reparameterization to accelerate training of deep neural networks. In *Advances in neural information processing systems*, pp. 901–909, 2016.

Shaw, P., Uszkoreit, J., and Vaswani, A. Self-attention with relative position representations. In *Proceedings of the 2018 Conference of the North American Chapter of the Association for Computational Linguistics: Human Language Technologies, Volume 2 (Short Papers)*, pp. 464–468, 2018.

Tassa, Y., Doron, Y., Muldal, A., Erez, T., Li, Y., Casas, D. d. L., Budden, D., Abdolmaleki, A., Merel, J., Lefrancq, A., et al. Deepmind control suite. *arXiv preprint arXiv:1801.00690*, 2018.

Vaswani, A., Shazeer, N., Parmar, N., Uszkoreit, J., Jones, L., Gomez, A. N., Kaiser, Ł., and Polosukhin, I. Attention is all you need. In *Advances in neural information processing systems*, pp. 5998–6008, 2017.

Williams, R. J. and Zipser, D. A learning algorithm for continually running fully recurrent neural networks. *Neural computation*, 1(2):270–280, 1989.

Xu, D., Ruan, C., Korpeoglu, E., Kumar, S., and Achan, K. Self-attention with functional time representation learning. In *Advances in Neural Information Processing Systems*, pp. 15915–15925, 2019.

Yoon, J., Jordon, J., and Schaar, M. Gain: Missing data imputation using generative adversarial nets. In *International Conference on Machine Learning*, pp. 5689–5698, 2018.

Zaheer, M., Kottur, S., Ravanbakhsh, S., Poczos, B., Salakhutdinov, R. R., and Smola, A. J. Deep sets. In *Advances in neural information processing systems*, pp. 3391–3401, 2017.

Zhang, S., Guo, B., Dong, A., He, J., Xu, Z., and Chen, S. X. Cautionary tales on air-quality improvement in beijing. *Proceedings of the Royal Society A: Mathematical, Physical and Engineering Sciences*, 473(2205):20170457, 2017.